

Summary of WG6: Spin Physics

Emanuele R. Nocera

Rudolf Peierls Centre for Theoretical Physics

1 Keble Road, University of Oxford

OX1 3NP Oxford, United Kingdom

E-mail: emanuele.nocera@physics.ox.ac.uk

Silvia Pisano

INFN Laboratori Nazionali di Frascati

Via Enrico Fermi 40, 00044, Frascati, Italy

E-mail: silvia.pisano@lnf.infn.it

The working group on Spin Physics at the XXIV International Workshop on Deep-Inelastic Scattering and Related Subjects (DIS2016) witnessed a significant progress in the theoretical and experimental investigations aiming at unveiling the innermost structure of the proton. Results ranged from proton's one-dimensional representation to its multi-dimensional imaging. In this contribution, we summarize a selection of the topics discussed and of the results presented. For details, we refer to the individual contributions collected in the proceedings of this workshop.

XXIV International Workshop on Deep-Inelastic Scattering and Related Subjects

11-15 April, 2016

DESY Hamburg, Germany

1. Introduction

Nucleons, protons and neutrons, are those bound states which make up all nuclei, and hence most of the visible matter in the Universe. Understanding their fundamental structure and dynamics in terms of their partonic constituents - quarks and gluons - is currently one of the main challenges in hadron physics [1]. Such an understanding has been rooted in the theoretical framework provided by Quantum Chromodynamics (QCD), the field theory which describes the strong interaction among quarks and gluons [2]. The theory has been developed to match the experimental probe of nucleon structure, which consists in scattering nucleons off a beam of leptons, or of other nucleons, in a large-momentum transfer process. Following factorization [3], hadronic cross sections measured in sufficiently inclusive processes are described as a convolution between a short-distance part - that encodes information on the hard interactions of partons in the form of perturbative computable, process-dependent kernels - and a long-distance part - that encodes information on the longitudinal momentum structure of the nucleon in the form of universal parton distribution functions (PDFs).

Despite this framework has been tremendously successful in the quantitative description of a wealth of experimental data measured by a number of facilities around the world, some fundamental aspects of the partonic structure of the nucleon are still rather poorly determined. The focus of hadron physics is currently on two such aspects: on the one hand, the understanding of the innermost nature of nucleon's total angular momentum in terms of the individual contributions of quarks, antiquarks and gluons [4]; on the other hand, the quest of a multi-dimensional picture of the nucleon, in which parton's transverse momentum and spatial position are taken into account [5].

These two aspects are strictly entwined with each other, as it has become clear for instance in the decomposition of the nucleon total angular momentum, of which a possible realization [6] in terms of its quark and gluon spin, $\Delta\Sigma$ and ΔG , and quark and gluon orbital momentum, \mathcal{L}_q and \mathcal{L}_g , is

$$\frac{1}{2} = \frac{1}{2}\Delta\Sigma(\mu^2) + \Delta G(\mu^2) + \mathcal{L}_q(\mu^2) + \mathcal{L}_g(\mu^2), \quad (1.1)$$

where μ^2 is the factorization scale. In principle one would like to be able to measure each term in Eq. (1.1), or at least a combination of them.¹ While $\Delta\Sigma$ and ΔG , which encode the information on the one-dimensional (1-D) spin structure of the proton, can be related to the longitudinally polarized PDFs, \mathcal{L}_q and \mathcal{L}_g , which encode the information on the multi-dimensional structure of the proton, should be related to some different objects. In principle, the distribution of partons inside a nucleon, as a simultaneous function of their longitudinal momentum fraction x , transverse momentum \mathbf{k}_T and impact-parameter space \mathbf{b}_T , is encoded in the five-dimensional (5-D) Wigner distribution $W(x, \mathbf{k}_T, \mathbf{b}_T)$. However, this cannot be accessed in the experiment. Integrating $W(x, \mathbf{k}_T, \mathbf{b}_T)$ in \mathbf{b}_T leads to the three-dimensional (3-D) transverse momentum dependent PDFs (TMDs), which are instead measurable quantities (typically in semi-inclusive processes). Note that a further integration of the TMDs in \mathbf{k}_T leads to the usual 1-D PDFs. Otherwise, integrating $W(x, \mathbf{k}_T, \mathbf{b}_T)$ in \mathbf{k}_T , then Fourier transforming the \mathbf{b}_T dependence into the Mandelstam variable $-t$, and finally extrapolating from zero to finite skewness ξ leads to the 3-D generalized parton

¹Note that the decomposition provided by Eq. (1.1) is not unique. What should be the decompositions that lead to gauge-invariant, physically meaningful terms (and in which sense these are measurable) are discussed in Ref. [7].

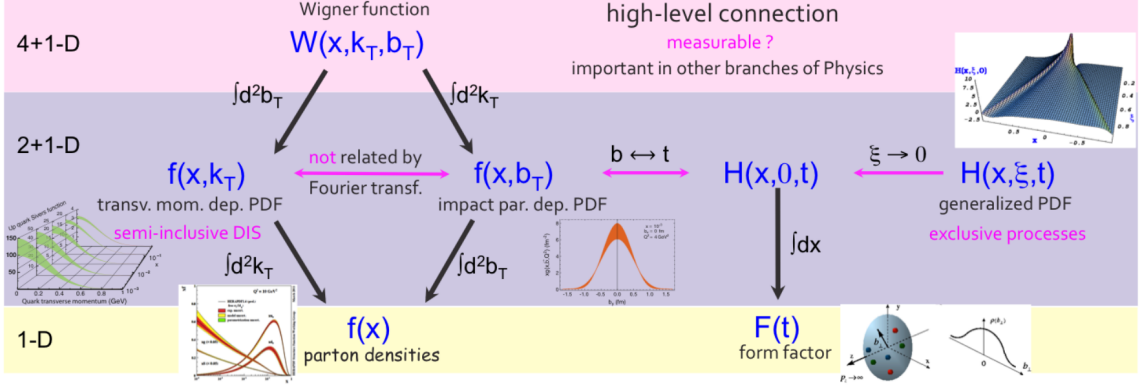


Figure 1: Connections among different functions describing the distribution of partons inside the proton. The functions given here are for unpolarized partons in an unpolarized proton; analogous relations hold for polarized quantities. The figure is taken from Ref. [9].

distribution functions (GPDs), see Fig. 1. These are measurable objects too (typically in exclusive processes), and may be related to the quark and gluon orbital momentum [8].

The working group on Spin Physics (WG6) at the XXIV International Workshop on Deep-Inelastic Scattering and Related Subjects (DIS2016) addressed recent theoretical and experimental developments in hadron physics, including the subjects outlined above. Almost fourteen hours, divided into eight sessions, were dedicated to presentations and discussions. Invited overview talks were also called for. An additional two-hour session, joint with the working group on Future Experiments (WG7), was organized to focus on prospective developments in spin physics, connected to future experimental facilities. A total of thirty-eight talks were presented.

In this contribution, we summarize some selected results: in Sec. 2, we discuss the 1-D representation of the longitudinal spin structure of the nucleon, while in Sec. 3 we address the 3-D mapping of the nucleon, focusing on TMDs and GPDs. Further details on each topic can be found in the individual contributions in these proceedings.

2. 1-D representation of the longitudinal nucleon spin structure

The first two terms in Eq. (1.1) represent the fraction of the nucleon spin carried by quarks and gluons respectively. Provided that the longitudinally polarized PDFs of the proton

$$\Delta f(x, \mu^2) \equiv f^\uparrow(x, \mu^2) - f^\downarrow(x, \mu^2) \quad (2.1)$$

are defined as the net momentum densities of partons (f denotes either a quark q , an antiquark \bar{q} , or a gluon g) with spin aligned along (\uparrow) or opposite (\downarrow) the polarization of the parent nucleon, $\Delta\Sigma$ and ΔG are then defined as their first moments

$$\Delta\Sigma(\mu^2) = \sum_{q=u,d,s} \int_0^1 dx [\Delta q(x, \mu^2) + \Delta\bar{q}(x, \mu^2)], \quad \Delta G(x, \mu^2) = \int_0^1 dx \Delta g(x, \mu^2). \quad (2.2)$$

The dependence of the PDFs on the factorization scale μ can be obtained as a perturbative solution of the DGLAP evolution equations [10], and the coefficients of the corresponding splitting functions have been computed up to next-to-next-to-leading order (NNLO) accuracy very recently [11].

The dependence of the PDF on the proton momentum fraction x carried by the parton is non-perturbative, and must be determined from the data. This is supplemented with some theoretical requirements, which include: positivity, *i.e.* PDFs must lead to positive cross sections; integrability, *i.e.* the nucleon matrix element of the axial current must be finite for each flavor; SU(2) and SU(3) flavor symmetry, *i.e.* the first moments of the nonsinglet \mathcal{C} -even PDF combinations are related to the baryon octet β -decay constants, whose values are well measured [12]. Recent theoretical and experimental progress in the determinations of the PDFs was extensively reported in WG6.

On the theoretical side, the available sets of longitudinally polarized PDFs of the proton differ among each other for the procedure used to determine PDFs from the data, for the data set included, and for the details of the QCD analysis, see *e.g.* Chap. 3 in Ref. [13] for a review.

As far as the procedure is concerned, three different approaches are being used. The first is based on simple polynomials for PDF parametrization and on standard Hessian or Lagrange multiplier techniques for PDF uncertainty estimates. The second is based on neural networks for PDF parametrization and Monte Carlo sampling for PDF uncertainty estimates. The third combines the two approaches, keeping simple polynomials for PDF parametrization and Monte Carlo sampling for PDF uncertainty estimates. Monte Carlo sampling techniques have the advantage to generate fits of PDFs with statistically rigorous uncertainties, while neural networks allow for a reduction of the bias associated to the choice of the parametrization. Among recent fits, those from the DSSV family [15, 16, 17] are based on the first approach, those from the NNPDF collaboration [18, 19] are based on the second and that from the JAM collaboration [20] is based on the third.

As far as the data set is concerned, the bulk of the experimental information in all the above-mentioned fits is provided by neutral current, photon-induced, inclusive deep-inelastic scattering (DIS). Very recent DIS measurements from COMPASS and JLAB have been included in a dedicated NNPDF analysis [21] as well as in the JAM PDF set. Because of the way the corresponding observables factorize, inclusive DIS data only constrain the total quark-antiquark combinations and, weakly, the gluon distribution via scaling violations. In order to overcome this issue, observables sensitive to individual quark and antiquark polarizations and receiving a leading contribution from gluon-initiated partonic subprocesses should be considered respectively. In the DSSV analysis the quark-antiquark PDFs are determined from semi-inclusive DIS (SIDIS), while the gluon PDF is determined from pion and jet production in polarized proton-proton (pp) collision at the Relativistic Heavy Ion Collider (RHIC); in the NNPDF analysis the quark-antiquark PDFs are determined from W boson production at RHIC, while the gluon PDF is determined from open-charm lepto-production in SIDIS and jet production at RHIC. The inclusion of SIDIS and pion production data requires the usage of poorly known fragmentation functions (FFs), which may spoil the accuracy of the ensued PDFs. Overall, RHIC data were demonstrated to point towards a sizable, positive gluon polarization in the proton [17, 19], and a sizable asymmetry of the polarized sea quarks [22], though these conclusions hold only in the rather limited region covered by data, $0.05 \lesssim x \lesssim 0.5$.

As far as the details of the QCD analysis are concerned, the DSSV, NNPDF and JAM PDF sets are determined in the $\overline{\text{MS}}$ scheme at next-to-leading order (NLO) accuracy.² In the JAM analysis, particular attention was put in the inclusion of finite- μ^2 and nuclear corrections relevant for JLAB kinematics; flavor-separated twist-3 contributions and the d_2 moment of the nucleon were also

²A NNLO QCD analysis of longitudinally polarized PDFs has been performed very recently, see Ref. [14].

determined. Although all the available PDF sets are determined at fixed order in the perturbative QCD expansion, resummed PDF fits are in principle possible [23], and threshold resummation for open-charm production at COMPASS was specifically discussed [24]. A valuable input on the determination of PDFs may come from nonperturbative models of nucleon structure [25], and, more and more promisingly, from first principle computations in lattice QCD [26].

On the experimental side, a wealth of new experimental data was illustrated.

The COMPASS collaboration presented new measurements of the deuteron longitudinal double spin asymmetry A_1^d and of the deuteron spin-dependent structure function g_1^d in DIS [27]. These data sets provide twice the precision of earlier COMPASS measurements and complement the analogous results for protons [28]. The COMPASS collaboration also presented a new analysis of the proton longitudinal spin asymmetry, A_1^p , and structure function, g_1^p , at low values of x and μ^2 in two-dimensional bins of various kinematic variables [29]. These data sets point towards a first evidence of positive spin effects at low x , which seems to be independent of the kinematics.

The PHENIX collaboration presented a new measurement of the double spin asymmetry for mid-rapidity neutral pion production in polarized pp collisions at a center-of-mass energy $\sqrt{s} = 510$ GeV [30]. This data set confirms a positive contribution of the gluon polarization to the proton spin, consistent with the finding from earlier measurements of pion and jet asymmetries; it also extends the sensitivity to ΔG down to $x \sim 0.01$ into a currently unexplored region. The PHENIX collaboration also reported on the double helicity asymmetry for inclusive J/Ψ production at forward rapidity in $\sqrt{s} = 510$ GeV polarized pp collisions [31]. Because J/Ψ particles are predominantly produced through gluon-gluon scattering, this data set is a further handle on ΔG , especially in the low x region, provided that the mechanism of J/Ψ production is clarified. The PHENIX collaboration also presented forward- and mid-rapidity measurements for W^\pm/Z production in polarized pp collisions [32]. This data set will provide further insight into antiquark polarized PDFs.

The STAR collaboration presented first dijet asymmetry measurements in polarized pp collisions at $\sqrt{s} = 500$ GeV and $\sqrt{s} = 510$ GeV [33]. This data set complements earlier STAR measurements on single-jet production, and will extend the current constraints on ΔG down to $x \sim 0.01$.

Despite all these achievements, the lack of experimental information over a wide range of x and μ^2 seriously limits the accuracy with which $\Delta\Sigma$ and ΔG in Eq. (1.1) can be determined [34]. Brand new facilities, such as the proposed high-energy, polarized Electron-Ion Collider (EIC) [35] will be required to definitely unveil their size with few percent accuracy [36, 37].

3. 3-D mapping of the nucleon

Once the 1-D representation of the nucleon structure is extended to a full 3-D imaging, a plethora of new phenomena emerge, connected to the non-trivial parton dynamics in the hadrons.

A first 3-D representation of the nucleon follows from the combination of the electromagnetic form factor and the PDF. The former describes the transverse distribution of the nucleon charge and magnetization, while the latter encodes the information on how the nucleon momentum is shared among its constituents in the longitudinal direction. The combination of the two leads to the GPDs, which describe the correlation among the parton transverse position and their momentum fraction (see Fig. 1). At leading twist, four different GPDs describe the nucleon for each quark flavor (in the *chiral-even* sector), depending on the occurrence or not of a spin flip in the quark

after the interaction with the hard probe [8]. They are usually accessed through deeply-virtual Compton scattering (DVCS), a hard exclusive process consisting in the electro-production of a *real* photon off a nucleon target. From a theoretical point of view, DVCS is described through the so-called *handbag* diagram, where the hard, perturbative dynamics describing the interaction of the struck quark with the exchanged virtual photon is factorized out of the soft, long-range dynamics describing the hadronic bound state. Such a soft, nonperturbative part is encoded in the GPDs: they depend on the fraction x of the nucleon momentum carried by the interacting quark, on the four-momentum $-t$ exchanged between the electron and the proton, and on its transverse fraction ξ .

The analysis of the DVCS cross-section $-t$ -slope provides a mapping of the nucleon size as a function of the fraction x considered, leading to an actual *transverse nucleon imaging*. While high- x , valence quarks seem to be confined at the center of the nucleon, low- x contributions seem to be spread at the periphery, resulting in a larger nucleon size once the low- x region is explored. A recent measurement by COMPASS on the 2012 pilot run has been reported, which extends the previous measurements by H1 and ZEUS [39, 40, 41] in the low- x region. Furthermore, the latest JLab data from Hall-A [42, 43] and Hall-B [44] cover with unprecedented precision the high- x domain [45]. Finally, a dedicated beam time for DVCS measurements with COMPASSII is foreseen for 2016-2017, which will provide further constraint on the DVCS cross section in the low- x region.

Depending on the polarization degrees of freedom active in the DVCS process, different GPDs can be accessed. Some of the GPDs reduce, in the forward limit, to the usual 1-D PDFs. The analysis of the $-t$ dependence of these GPDs can then shed light on how the related charges are distributed inside the nucleon. A recent measurement by the Hall-B (CLAS) Collaboration realized on a longitudinally-polarized NH_3 target [46, 47] compared the $-t$ dependence for the beam-spin asymmetry (related to the GPD H , that reduces to the electric charge) to the target-spin asymmetry (related to the GPD \tilde{H} , that reduces to the axial charge). The $-t$ dependence observed for the beam-spin asymmetry is steeper than that for the target-spin asymmetry, thus suggesting that the axial charge is focused inside the nucleon volume more than the electric one.

A complementary 3-D representation of the nucleon is provided, in the momentum space, by transverse-momentum-dependent parton distributions (TMD-PDFs). These are a generalization of PDFs, which include an additional dependence on a small component k_T of the parton momentum, transverse to the virtual photon direction. Like PDFs and GPDs, TMDs also depend on the usual longitudinal momentum fraction x , and are accessed through hard processes, in particular in SIDIS, electron-positron annihilation and pp collisions.

In SIDIS, in addition to the outgoing electron, at least one hadron is detected. The kinematic of the latter is then used to explore the dynamics characterizing the struck quark motion inside the nucleon, by relating the transverse hadron momentum P_T to the (not accessible) parton k_T . In order to describe the mechanism leading to the formation of the final hadron through the electron scattering off a given target, a second, nonperturbative, object is needed in the cross section, the transverse-momentum-dependent fragmentation functions (TMD-FFs). At leading twist, the SIDIS cross section can be expressed in terms of up to eighteen structure functions (with each structure function being a convolution over k_T of a TMD-PDF and a TMD-FF) [48]. Each of these structure functions can be accessed through specific combinations of polarization degrees of freedom (*e.g.*, unpolarized, longitudinally polarized or transversely polarized beam or target).

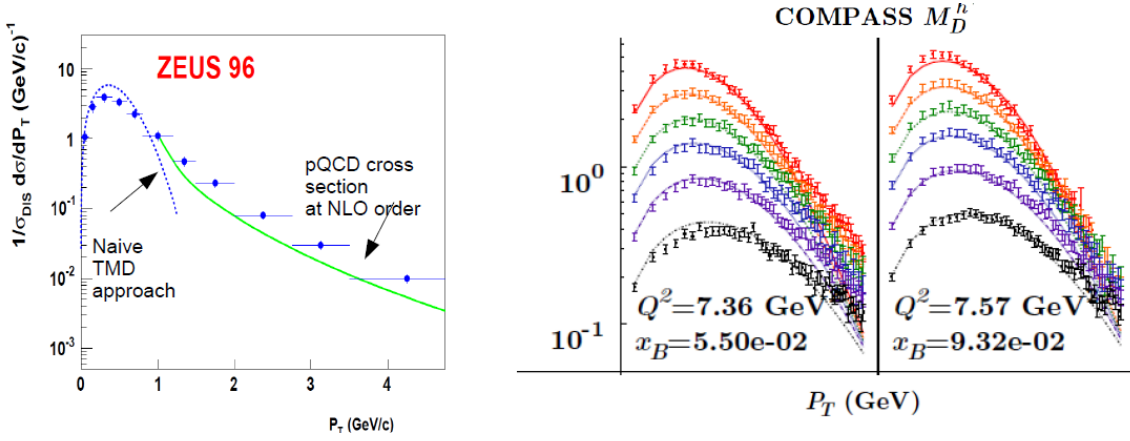


Figure 2: The dependence of the DIS cross section on the hadron transverse momentum P_T for two different kinematics regimes. ZEUS data on the left plot show deviation from the Gaussian shape in the high- P_T region, while COMPASS multiplicities are well reproduced in the right plots.

The unknown k_T dependence needed to disentangle the two nonperturbative functions is an essential object in describing the parton dynamics. However, it is not directly accessible, so constraints on it can only come through phenomenological tests on the different hypothesis on its shape. Furthermore, providing theoretical predictions of cross sections for hadronic processes over the whole P_T range explored by experiments is a highly nontrivial task. Fixed-order pQCD fails to describe low- P_T data, and the cross section tail at large P_T seems to deviate from the usual Gaussian ansatz, see Fig. 2. A recent review on the transverse spin phenomenology can be found in Ref. [49].

SIDIS data have been collected during the last decades by several experiments, providing first constraints on the various TMD-PDFs and TMD-FFs. Recently, an extended lever-arm in Q^2 has been explored, thanks to simultaneous measurements by COMPASS in the low- x region and by HERMES and JLAB in the medium and high- x regime. Among all the various observables, the transverse target-spin asymmetry A_{UT} plays a crucial role, since it provides access to the Collins and Sivers amplitudes. The former is essential since it is one of the possible ways to access the transversity PDF $h_1(x)$: indeed, being chiral-odd, $h_1(x)$ cannot be accessed through inclusive DIS. Instead, it has to appear in observables coupled to a second chiral-odd object, which is represented by the Collins function in SIDIS.

A comparison between the Collins modulation on the proton extracted by COMPASS [50] and HERMES [51] is shown in Fig. 3. The two sets of data cover different kinematic domains, and show a good agreement in the overlapping regions. By combining proton and deuteron data, a flavor separation can be achieved, possibly leading to the extraction of the transversity for the single quark flavors [52].

As far as electron-positron annihilation is concerned, first BELLE measurements of double differential cross sections of two charged pions and kaons as a function of the fractional energies of the two hadrons for any charge and hadron combination have been presented [53]. The ratios of these di-hadron cross sections for different charges and hadron combinations directly shed light on

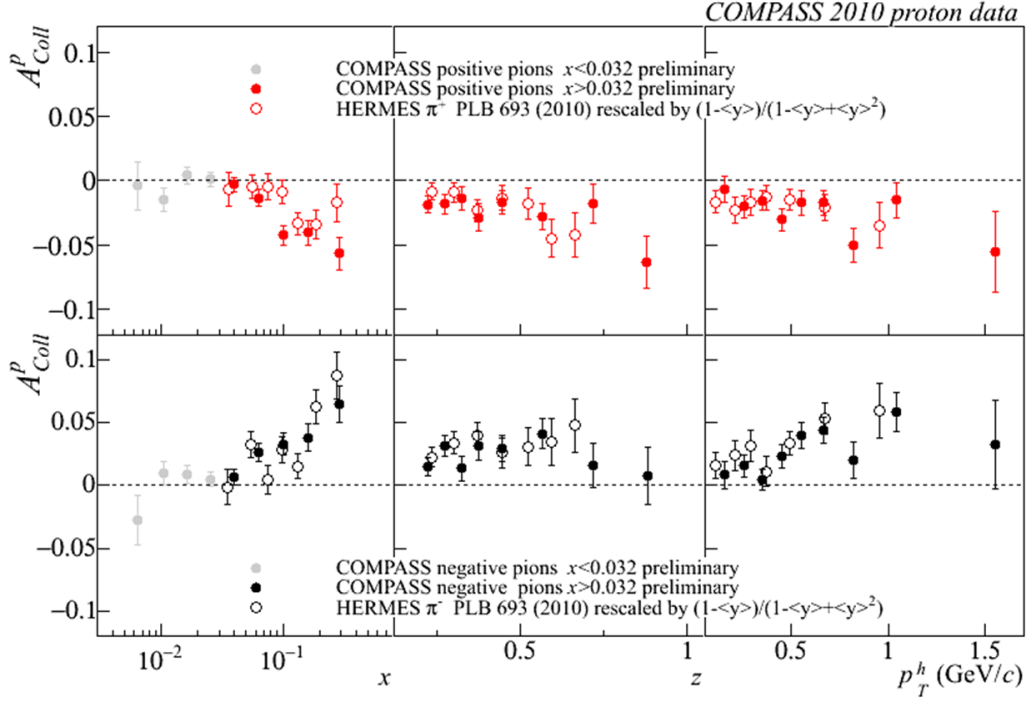


Figure 3: The Collins modulation of the proton, A_{Coll}^p , as a function of x , z and P_T for positive pions (top) and for negative pions (bottom) as extracted from COMPASS and HERMES [51].

the contributing TMD-FFs. For example, it was found that the ratio of same-sign pion pairs over opposite-sign pion pairs drops toward higher fractional energies, where disfavored fragmentation is expected to be suppressed.

Finally, significant progress has also been reported in pp collisions. Most importantly, a first measurement of the transverse single-spin asymmetry of Drell-Yan (DY) weak boson production in transversely polarized pp collisions at $\sqrt{s} = 500$ GeV by the STAR experiment has been discussed [54]. The measured observable is sensitive to the Sivers function f_{1T}^\perp [55], one of the TMDs which describes the correlation between the intrinsic transverse momentum of a parton and the spin of the parent proton. A general prediction following from Gauge invariance of QCD and QCD factorization formalism [56, 57] is that TMDs in general are not universal objects, but rather depend on the process under examination. For instance, the Sivers function is predicted [56] to have the opposite sign in SIDIS compared to processes with color changes in the initial state and a colorless final state, such as $pp \rightarrow DY/W^\pm/Z^0$. Results for the transverse spin asymmetry for weak boson production, A_N are shown in Fig. 4 as a function of the boson rapidity y^W . Theoretical predictions based on the KQ [58] and on the EIKV [59] models are also displayed. The latter includes TMD evolution effects, and predicts the largest effects of TMD evolution among many TMD-evolved theoretical computations. It was shown [54] that a combined fit to W^+ and W^- transverse spin asymmetries based on the KQ model leads to a significantly better χ^2 if a sign-change of the Sivers function is assumed, see Fig 5. Therefore, provided TMD evolution effects are small, the current data seems to favor theoretical models that include a change of sign for the Sivers function in

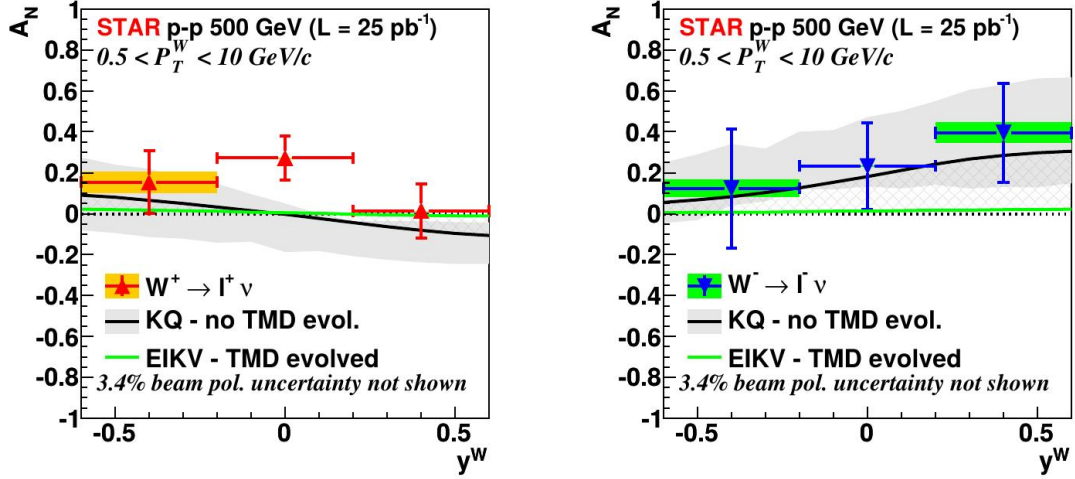


Figure 4: The transverse single-spin asymmetry A_N for W^\pm and Z^0 boson production measured by STAR in pp collisions at $\sqrt{s} = 500 \text{ GeV}$ with a recorded luminosity of 25 pb^{-1} . The solid gray bands represent the uncertainty on the KQ model [58] due to the unknown sea quark Sivers function. The crosshatched region indicates the current uncertainty in the theoretical predictions due to TMD evolution. This figure is taken from Ref. [54].

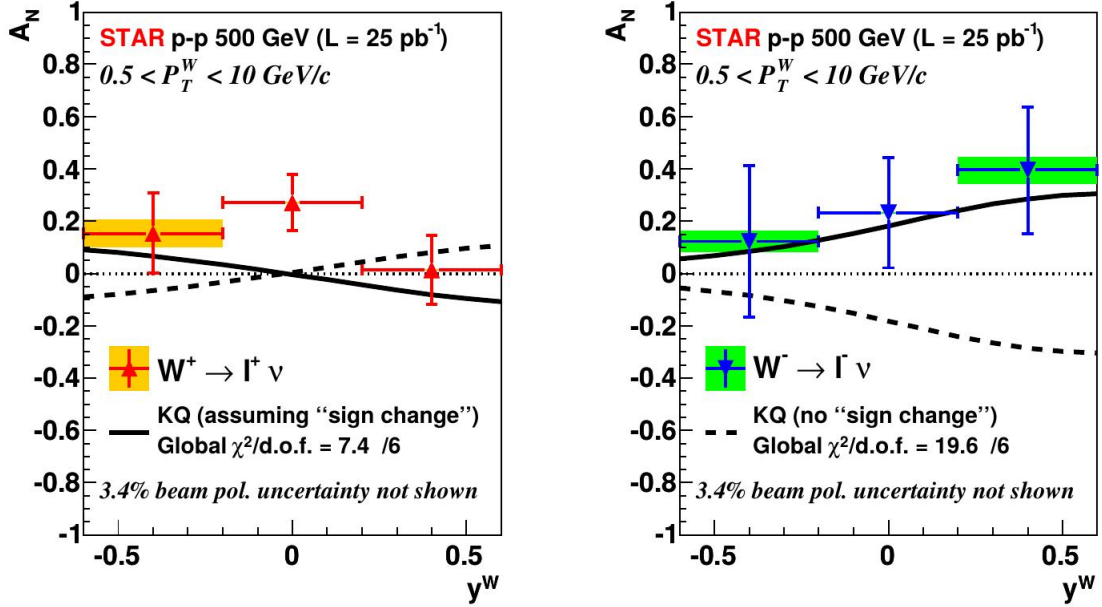


Figure 5: The transverse single-spin asymmetry A_N for W^+ (left plot) and W^- (right plot) boson production as a function of the boson rapidity y^W compared to the non TMD-evolved KQ model [58], assuming (solid line) or excluding (dashed line) a sign change in the Sivers function. Figure taken from Ref. [54].

comparison to observations in SIDIS measurements.

Acknowledgements

We were glad to serve as conveners of the DIS2016 Spin Working Group. We would like to warmly thank all the speakers for their interesting talks and discussions, and the local organizing committee for arranging a fruitful conference and a pleasant stay in Hamburg. E.R.N. is supported by a STFC Rutherford Grant ST/M003787/1.

References

- [1] A. W. Thomas and W. Weise, “The Structure of the Nucleon,” Berlin, Germany: Wiley-VCH (2001).
- [2] D. J. Gross and F. Wilczek, Phys. Rev. D **8** (1973) 3633, Phys. Rev. D **9** (1974) 980.
- [3] J. C. Collins, D. E. Soper and G. F. Sterman, Adv. Ser. Direct. High Energy Phys. **5** (1989) 1.
- [4] C. A. Aidala, S. D. Bass, D. Hasch and G. K. Mallot, Rev. Mod. Phys. **85** (2013) 655.
- [5] M. Anselmino, M. Guidal and P. Rossi Eur. Phys. J. A **52** (2016) 164.
- [6] R. L. Jaffe and A. Manohar, Nucl. Phys. B **337** (1990) 509.
- [7] E. Leader and C. Lorcé, Phys. Rept. **541** (2014) 163.
- [8] S. Boffi and B. Pasquini, Riv. Nuovo Cim. **30** (2007) 387.
- [9] E. C. Aschenauer *et al.*, arXiv:1501.01220 [nucl-ex].
- [10] G. Altarelli and G. Parisi, Nucl. Phys. B **126** (1977) 298.
- [11] S. Moch, J. A. M. Vermaseren and A. Vogt, Nucl. Phys. B **889** (2014) 351.
- [12] K. A. Olive *et al.* [Particle Data Group Collaboration], Chin. Phys. C **38** (2014) 090001.
- [13] E. R. Nocera, *Unbiased spin-dependent Parton Distribution Functions*, PhD thesis (2014).
- [14] F. Taghavi-Shahri *et al.* Phys. Rev. D **93** (2016) no.11, 114024.
- [15] D. de Florian, R. Sassot, M. Stratmann and W. Vogelsang, Phys. Rev. Lett. **101** (2008) 072001.
- [16] D. de Florian, R. Sassot, M. Stratmann and W. Vogelsang, Phys. Rev. D **80** (2009) 034030.
- [17] D. de Florian, R. Sassot, M. Stratmann and W. Vogelsang, Phys. Rev. Lett. **113** (2014) no.1, 012001.
- [18] R. D. Ball *et al.* [NNPDF Collaboration], Nucl. Phys. B **874** (2013) 36.
- [19] E. R. Nocera *et al.* [NNPDF Collaboration], Nucl. Phys. B **887** (2014) 276.
- [20] N. Sato *et al.* [JAM Collaboration], Phys. Rev. D **93** (2016) no.7, 074005.
- [21] E. R. Nocera, J. Phys. Conf. Ser. **678** (2016) no.1, 012030.
- [22] E. R. Nocera, PoS DIS **2014** (2014) 204.
- [23] F. M. Ringer, *Threshold Resummation and Higher Order Effects in QCD*, PhD thesis (2015).
- [24] C. Uebler, A. Schäfer and W. Vogelsang, Phys. Rev. D **92** (2015) no.9, 094029.
- [25] E. R. Nocera, Phys. Lett. B **742** (2015) 117.
- [26] C. Wiese, these proceedings.
- [27] M. Wilfert, these proceedings.

- [28] C. Adolph *et al.* [COMPASS Collaboration], Phys. Lett. B **753** (2016) 18
- [29] S. Nunes, these proceedings.
- [30] A. Adare *et al.* [PHENIX Collaboration], Phys. Rev. D **93** (2016) no.1, 011501.
- [31] A. Adare *et al.*, arXiv:1606.01815 [hep-ex].
- [32] A. Adare *et al.* [PHENIX Collaboration], Phys. Rev. D **93** (2016) no.5, 051103
- [33] S. Ramachandran, these proceedings.
- [34] E. R. Nocera, Int. J. Mod. Phys. Conf. Ser. **40** (2016) 1660016
- [35] A. Accardi *et al.*, arXiv:1212.1701 [nucl-ex].
- [36] E. C. Aschenauer *et al.*, Phys. Rev. D **92** (2015) no.9, 094030, see also these proceedings.
- [37] R. D. Ball *et al.* [NNPDF Collaboration], Phys. Lett. B **728** (2014) 524
- [38] M. Diehl, Phys. Rept. **388** (2003) 41
- [39] S. Chekanov *et al.* [ZEUS Collaboration], JHEP **0905** (2009) 108
- [40] A. Aktas *et al.* [H1 Collaboration], Eur. Phys. J. C **44** (2005) 1
- [41] F. D. Aaron *et al.* [H1 Collaboration], Phys. Lett. B **681** (2009) 391
- [42] C. M. Camacho *et al.* [Jefferson Lab Hall A and Hall A DVCS Collaborations], Phys. Rev. Lett. **97** (2006) 262002
- [43] M. Defurne *et al.* [Jefferson Lab Hall A Collaboration], Phys. Rev. C **92** (2015) no.5, 055202
- [44] H. S. Jo *et al.* [CLAS Collaboration], Phys. Rev. Lett. **115** (2015) no.21, 212003
- [45] S. Niccolai, these proceedings.
- [46] E. Seder *et al.* [CLAS Collaboration], Phys. Rev. Lett. **114** (2015) no.3, 032001 Addendum: [Phys. Rev. Lett. **114** (2015) no.8, 089901]
- [47] S. Pisano *et al.* [CLAS Collaboration], Phys. Rev. D **91** (2015) no.5, 052014
- [48] M. Anselmino *et al.* Phys. Rev. D **83** (2011) 114019
- [49] M. Boglione and A. Prokudin, Eur. Phys. J. A **52** (2016) no.6, 154
- [50] C. Adolph *et al.* [COMPASS Collaboration], Phys. Lett. B **744** (2015) 250
- [51] A. Airapetian *et al.* [HERMES Collaboration], Phys. Lett. B **693** (2010) 11
- [52] A. Martin, F. Bradamante and V. Barone, Phys. Rev. D **91** (2015) no.1, 014034
- [53] R. Seidl *et al.* [Belle Collaboration], Phys. Rev. D **92** (2015) no.9, 092007
- [54] L. Adamczyk *et al.* [STAR Collaboration], Phys. Rev. Lett. **116** (2016) no.13, 132301
- [55] D. W. Sivers, Phys. Rev. D **41** (1990) 83, D **43** (1991) 261.
- [56] J. C. Collins, Phys. Lett. B **536** (2002) 43
- [57] P. Mulders, these proceedings.
- [58] Z. B. Kang and J. W. Qiu, Phys. Rev. Lett. **103** (2009) 172001
- [59] M. G. Echevarria, A. Idilbi, Z. B. Kang and I. Vitev, Phys. Rev. D **89** (2014) 074013